Granular Betas and Risk Premium Functions

This version: October 26, 2022

Tim Bollerslev[a,*], Andrew J. Patton[b], Rogier Quaedvlieg[c]

[a] *Department of Economics, Duke University, NBER and CREATES*
[b] *Department of Economics, Duke University*
[c] *European Central Bank*

Abstract

We propose new refined measures of the local covariation between the return on an asset and a risk factor. Our proposed "granular betas" generalize the notion of up- and down-side betas to multi-factor functional measures of covariation. We then show how the resulting granular beta functions may be used in the estimation of new "risk premium functions." Implementing the proposed new methods with a large cross-section of U.S. equity returns, we find significant evidence against the traditional (non-granular) CAPM, the Fama-French three and five-factor models, and the Fama-French-Carhart model in favor of the new granular versions of these models. Our empirical results also provide new insights into where in the "factor space" the compensation for exposures to systematic risks is mostly earned.

Keywords: Cross section of expected returns, factor models, downside risk, granular betas, risk premium functions.

J.E.L. codes: G11, G12, C58.

---

[*] We thank participants at various conferences and seminars for their useful comments and suggestions on earlier versions of the paper. The second author also thanks UNSW Business School, where part of this work was completed, for their hospitality. The opinions in this paper are those of the authors and do not necessarily reflect the views of the European Central Bank or the Eurosystem.

[*] Corresponding author: Department of Economics, Duke University, Durham, NC 27708; 919-660-1846; boller@duke.edu.

1. Introduction

Linear factor models, starting with the CAPM (Sharpe, 1964; Lintner, 1965) and its many subsequent generalizations (Fama and French, 1992; Carhart, 1997; Fama and French, 2015, amongst many others), remain ubiquitous in empirical asset pricing. Their ease of implementation and interpretation makes the models an especially useful, if imperfect, tool for understanding systematic risks and explaining cross-sectional variation in returns. The advantages of linear models notwithstanding, the simplicity of such models can also mask potentially important non-linear dependencies and pricing. For example, prospect theory (Kahneman and Tversky, 1979) and disappointment aversion (Gul, 1991), imply that investors care more deeply about losses than gains, and as a result up- and down-side risks need not be priced the same. Other work on preferences over higher-order moments (Kimball, 1993) and rare disasters (Wachter, 2013) similarly suggest that investors price tail risks more dearly than "modal" risks near the center of the distribution. Capturing such non-linear features requires either the addition of new factors, or new methods.

Rather than adding to the population of Cochrane's (2011) already large "factor zoo," we instead propose to refine the way in which we measure the risk exposures to a given set of existing factors. Drawing on recent developments in high frequency financial econometrics, we increase the information content of a given factor model by measuring the covariation between an asset and a factor in a "granular" fashion. To do so, we propose new measures of dependence designed to locally capture the strength of the covariance between an asset and a factor across the entire support of the factor return. The resulting new "granular betas" generalize the up- and down-side market betas of Ang, Chen and Xing (2006) to allow for multiple factors and to provide a much more refined look at the inherent dependencies between an asset and a given set of factors.

To illustrate the idea, Figure 1 plots the averages of the traditionally estimated betas for all firms in the "Hi-Tech" and "Utilities" industries relative to the grand average of

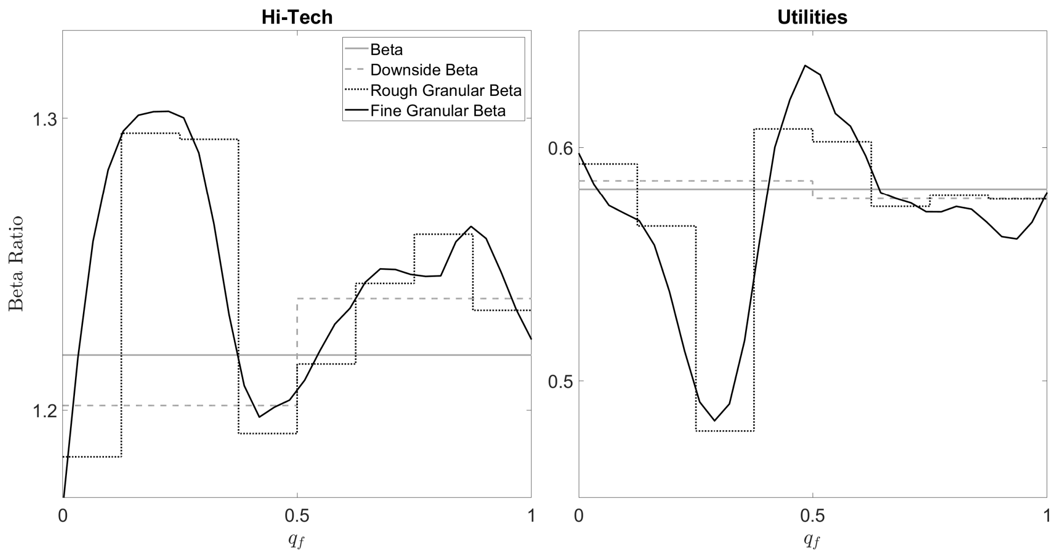

Figure 1: **Relative granular betas for hi-tech and utility stocks**. The figure shows the average CAPM, downside, and granular market betas of "Hi-Tech" and "Utilities" stocks relative to the corresponding average betas for all firms in our sample. The ratios are plotted as a function of the quantiles of the market return, q_f.

the estimated betas for all of the stocks in our sample.[1] As the estimated ratios for the traditional betas, labeled "Beta" in the figure, show, hi-tech firms tend to have betas in excess of the market average, while the betas of utility stocks tend to be lower. Looking at the dashed lines labeled "Downside Beta," which report the ratios of the average estimates of the up- and down side betas for the two industries relative to the up- and down-side betas for all stocks, we see that even though the down-side betas for hi-tech stocks are generally larger than the down-side beta for the average stock, as seen by the dashed line for the quantiles of the market return q_f below 0.5, the up-side betas for hi-tech stocks are even larger in a relative sense. Meanwhile, the up- and down-side betas for utility stocks are both very similar in a relative sense to the average up- and down-side betas for all stocks. The new "Rough" and "Fine" granular beta estimates tell a somewhat different and more nuanced story.[2] In particular, while the betas for

[1]Section 4.1 below provides a more detail description of the data. The industry definitions are based on the 10-SIC classifications on Ken French's website. We will return to these same two industries in our empirical analyses below.

[2]The terms "Rough" and "Fine" refer to the granularity used in calculating the betas, as discussed in more detail below. The estimates shown in the figure rely on $G = 8$ and $G = 64$ such q_f-based regions.

hi-tech firms are generally higher than the betas for most other stocks, in extreme down markets, when q_f is close to zero, hi-tech stocks tend to move less with the market than their CAPM and downside betas would suggest. Conversely, for utility stocks the more pronounced deviations from the more traditional beta estimates occur near the center of the return distribution.

These more granular characterizations of the risks also hold the promise of more accurate asset price predictions compared to the standard linear factor models, which effectively treat the granular beta functions as constants, or downside versions of said models, which allow for separate pricing of up- and down-side betas. However, the use of a function or a set of functions, as opposed to a scalar or a vector, to describe the risk exposures also complicates the estimation of the compensation for risks, or risk premiums. To overcome this hurdle, we rely random field regressions (Cohen and Jones, 1969), in which we regress the returns on a cross-section of assets on the granular beta functions to estimate new "risk premium functions." Our approach may be seen as a natural extension of the traditional Fama-MacBeth approach for estimating risk premiums in linear factor models to the new granular setting. We further show how these functional regressions may be meaningfully estimated using sieve approximations (Andrews, 1991; Newey, 1997; Chen, 2007), and easily implemented empirically by standard OLS procedures. We also demonstrate how this same estimation approach may be used to test various economic hypotheses related to the shape of the estimated risk premium functions, including that the functions are flat, as implied by traditional factor models.

Implementing the new procedures with U.S. equity return data over the period from 1963 to 2020, we find that the out-of-sample fit of a CAPM using granular betas is significantly better than the standard non-granular version and the downside version of the model. We further trace the improvements to the premium for covariation with the market factor being especially large in the left most part of its distribution, consistent with the idea that downside tail risk is priced more dearly by investors. The use of granular factor betas similarly improves on the out-of-sample performance of the Fama and French (1992) three-factor model, the Carhart (1997) four-factor model, and the five-factor model of Fama and French (2015). The improvements in fit again accrue because the shape of the best-fitting risk premium functions for many of the factors are significantly different from being flat.

The rest of the paper is organized as follows. We begin in Section 2 by placing our work in context of the extant literature. Section 3 presents the key ideas and new estimation and inference procedures. Section 4 discusses our main empirical findings. Section 5 considers various extensions and applications. Section 6 concludes. Some more detail explanations and supportive empirical analyses are deferred to the Appendix. Additional robustness checks and empirical results are also provided in an online Supplemental Appendix.

2. Related literature

Our work relates to several strands of the asset pricing literature. The most closely related papers are perhaps the aforementioned study by Ang et al. (2006) on the downside CAPM, and the more recent work by Bollerslev, Patton and Quaedvlieg (2022b), who refine the up- and down-side betas to also condition on the sign of the return on the individual assets. In contrast to both of these studies, however, which rely on fixed thresholds at zero for partitioning the betas, our method allows us to determine where, in the support of the factors, risk exposures earn greater or lesser compensation, for example, in the tails versus the center of the distribution. The related quantile spectral betas proposed by Baruník and Nevrla (2020) are also explicitly designed to focus on tail dependencies across different return horizons.

Our empirical finding that the estimated risk premium function for the market factor does indeed appear especially steep for the most left part of the support, also links our paper to earlier work on tails and the pricing of tail risks by Bollerslev and Todorov (2011), Kelly and Jiang (2014), Farago and Tedongap (2018) and Beason and Schreindorfer (2022), among others. Unlike these papers, however, we consider both single and multi-factor models. Chabi-Yo, Huggenberger and Weigert (2022) and Massacci, Sarno and Trapani (2021) consider the pricing of tail risks in the context of multi-factor models, with the former paper imposing a specific threshold where the "tails" begin and risk prices may differ, and the latter paper estimating a specific threshold. Instead, our approach deliberately relies on linear measures of risk, the proposed granular betas. Of course, by locally measuring the covariation, granular betas are also able to capture higher-moment dependence, as studied in Harvey and Siddique (2000), Dittmar (2002), Conrad, Dittmar and Ghysels (2013) and Langlois (2020) for example.

The way in which we operationalize the granular betas draws on work in high-frequency financial econometrics, with our estimates naturally interpreted as generalizations of the "realized betas" of Barndorff-Nielsen and Shephard (2004), used by Andersen, Bollerslev, Diebold and Wu (2006), Patton and Verardo (2012) among many others. The granular betas also formally, for increasingly finer partitions, encompass the jump and continuous betas defined and analyzed by Todorov and Bollerslev (2010) and Bollerslev, Li and Todorov (2016), and their multi-factor extensions recently developed Aït-Sahalia, Jacod and Xiu (2021) and Aleti (2022). Our estimates of the granular betas also builds on the notion of "realized semicovariances" of Bollerslev, Li, Patton and Quaedvlieg (2020), which entail separate covariances for the different quadrants of the real plane. However, instead of partitioning the two-dimensional plane into four regions, in our main analyses we instead partition the support of each of the factors into G consecutive non-overlapping segments. The resulting potentially "asymmetric" realized measures, thus resemble the "realized semivariances" of Barndorff-Nielsen, Kinnebrock and Shephard (2010) and Patton and Sheppard (2015). The estimates underlying our more elaborate multi-dimensional betas based on joint partitioning of the factors similarly resemble the "realized partial covariances" of Bollerslev, Medeiros, Patton and Quaedvlieg (2022a).

Our use of random field regressions and sieve approximation techniques also naturally links our study to recent work on machine learning methods in finance. For example, Freyberger, Neuhierl and Weber (2020) propose non-parametric sieve estimation of risk premiums on characteristics, while Kozak, Nagel and Santosh (2020) and Fan, Ke, Liao and Neuhierl (2022) propose various dimension reduction methods, including LASSO and PCA, to tractably incorporate the information from potentially hundreds of characteristics. Related, Cai, Fang and Xu (2022) explore the use of functional-coefficient panel data methods to estimate the betas in a factor model as non-parametric functions of macroeconomic variables. We differ from all of these papers in that we do not attempt to augment the factor models with information from firm characteristics or any other sources. Instead, we seek to enhance the explanatory power of existing linear factor models through the use of more refined measures of a given asset's covariation with established asset pricing factors.

The idea of partitioning the factor space to obtain additional information is also related to the concepts of random forests and regression trees used in the machine learning literature. Forecast techniques from machine learning have been used in a series of recent studies by Gu, Kelly and Xiu (2020), Bianchi, Büchner and Tamoni (2021), Bali, Goyal, Huang and Jiang (2022), and Li and Rossi (2022) to predict stock, Treasury bond, corporate bond, and mutual fund returns, respectively. Bryzgalova, Pelger and Zhu (2021) rely on decision trees in their construction of informative portfolios, or test assets, used in their estimation of a stochastic discount factor (SDF). Cong, Feng, He and He (2022) similarly rely on tree-based methods to generate basis portfolios for spanning the SDF. In contrast to all of these studies, which are based on "blind" data-driven procedures for determining non-linear dynamic dependencies or combining assets into portfolios, we start with a set of established risk factors. We then partition the factor loadings, or betas, into so-called granular betas based on the joint empirical distributions of the assets and the factors, in turn allowing for the estimation of new risk premium functions and asset specific "expected return functions."

3. Granular betas and the risk premium function

We begin by formally defining and discussing the "granular betas" and some of their theoretical properties. We then describe how these measures allow for the estimation of a "risk premium function." For simplicity of exposition, we focus most of the discussion on the simple one-factor case, and then extend to multi-factor models.

3.1. Main ideas and definitions

We denote the excess return on the factor and asset i as X and Y_i, respectively. Consider a set of G partitions of the support of the factor return, say $Q_1, ..., Q_{G-1}$, with $Q_0 \equiv -\infty$ and $Q_G \equiv \infty$. Let the j^{th} partition be denoted $\mathcal{G}_j = (Q_{j-1}, Q_j]$, for $j = 1, 2, ..., G$. We then define the granular covariance for asset i conditional on the factor return lying in partition $\mathcal{G}_j$ as:

$$\mathrm{GCov}(Y_i, X; \mathcal{G}_j) = \mathbb{E}[(Y_i - \mu_i)(X - \mu_x)|X \in \mathcal{G}_j]. \quad (1)$$

The granular betas are then simply obtained by normalizing the set of granular covariances with the factor variance:[3]

$$\mathrm{G}\beta_i(\mathcal{G}_j) \equiv \frac{\mathrm{GCov}(Y_i, X; \mathcal{G}_j)}{\sigma_x^2}. \quad (2)$$

Note that if the factor X refers to the excess return on the market, the probability weighted sum of the granular betas naturally equals the traditional CAPM beta:

$$\beta_i = \sum_{j=1}^{G} \mathrm{G}\beta_i(\mathcal{G}_j)\mathrm{Pr}[X \in \mathcal{G}_j].$$

[3] Alternatively, the granular covariances could be normalized by the "granular variance," $\mathbb{E}[(X - \mu_x)^2|X \in \mathcal{G}_j]$. This alternative would affect some of the shapes that obtain using the simpler normalization in (2), e.g., as discussed further below, the granular beta function obtained under the CAPM would no longer be a parabola.

Hence, in the one-factor setting with X equal to the market, the granular betas may be interpreted as an additive decomposition of the usual CAPM beta. Moreover, if the quantiles of the market factor are used to determine a set of equally likely partitions, so that $\Pr[X \in \mathcal{G}_j] = 1/G$ for all j, the usual CAPM beta is simply obtained as the equal-weighted average of the granular betas. Moreover, if we consider just $G = 2$ partitions, with the boundary at zero, we recover the up- and down-side betas of Ang et al. (2006).

To further appreciate what the granular betas estimate, it is instructive to consider their limit as the width of the partitions converges to zero, or $\Delta \to 0$:

$$\begin{aligned} \mathrm{G}\beta_i((x, x+\Delta]) &= \frac{\mathbb{E}[(Y_i - \mu_i)(X - \mu_x)|x < X \leq x + \Delta]}{\sigma_x^2} \\ &\to \frac{(\mathbb{E}[Y_i|X = x] - \mu_i)(x - \mu_x)}{\sigma_x^2} \equiv \mathrm{G}\beta_i^*(x). \end{aligned} \tag{3}$$

We will refer to this limiting function as the "granular beta function" in the sequel. The functional form of $\mathrm{G}\beta_i^*(x)$ reveals that granular betas are related to the conditional mean of the test asset given the factor. Analogous to the case with a finite number of partitions, the law of iterated expectations again implies that for the market factor, the expectation of this function reduces to the usual CAPM beta, that is, $\mathbb{E}[\mathrm{G}\beta_i^*(X)] = \beta_i$.

Of course, it is possible that the compensation earned for exposure to the factor X may differ across the support of the factor. As a case in point, existing empirical evidence suggests that market tail risk may be prized more dearly than "normal" risk corresponding to realizations of X closer to the center of its distribution. In other words, the risk premiums associated with the granular beta function $\mathrm{G}\beta_i^*(x)$ may depend on x. Specifically, let $\lambda(x)$ denote the "risk premium function" that characterizes how the compensation varies with x across the support of X. The expected return on Y_i may then be expressed as:

$$\mathbb{E}(Y_i) = \int_{-\infty}^{\infty} \lambda(x)\mathrm{G}\beta_i^*(x) f_X(x)dx, \tag{4}$$

where $f_X(\cdot)$ denotes the PDF of X.

To help further intuit the meaning of the granular betas and risk premium functions defined above, suppose that the traditional CAPM holds, so that the conditional mean of the return on Y_i satisfies $E[Y_i|X] = \beta_i X$, where X denotes the excess return on the market. Substituting this expression into equation (3) shows that the granular beta function implied by the CAPM is a parabola:

$$\mathrm{G}\beta_i^*(x) = \beta_i \frac{(x-\mu_x)^2}{\sigma_x^2}. \tag{5}$$

Moreover, as formally shown in Appendix A, for the expected return to be linear in β_i, the $\lambda(x)$ risk premium function cannot depend on x. In other words, for the traditional CAPM to hold, the lambda function must be constant across all values of x. We will refer to this as the lambda function being "flat" in the sequel.

Of course, there is overwhelming empirical evidence to suggest that the traditional CAMP does not hold empirically and that the granular beta function with respect to the market therefore does not resemble equation (5). To determine what the granular betas actually look like empirically, we turn next to their practical estimation.

3.2. Estimating granular betas

Drawing on the theory for realized semicovariances (Bollerslev et al., 2020), we estimate the time t granular beta for asset i with respect to factor X by:

$$\widehat{\mathrm{G}\beta}_{i,t,j} = \frac{\widehat{\mathrm{GCov}}_{i,t,j}}{\hat{\sigma}_{x,t}}, \tag{6}$$

where

$$\widehat{\mathrm{GCov}}_{i,t,j} = \sum_{s=t-S+1}^{t} (Y_s - \bar{Y}_t)(X_s - \bar{X}_t)\mathbf{1}\{X_s \in \mathcal{G}_j\}, \tag{7}$$

$$\hat{\sigma}_{x,t} = \sum_{s=t-S+1}^{t} (X_s - \bar{X}_t)^2, \tag{8}$$

and $\bar{X}_t$ and $\bar{Y}_t$ refer to the sample means of X_t and Y_t over the previous S periods.[4] This construction directly mirrors the approach in the burgeoning high-frequency volatility literature, in which the variance over fixed time-intervals is estimated from the sums of within interval more finely sampled squared returns, rather than their averages. As such, the realized beta defined by Barndorff-Nielsen and Shephard (2004) is simply obtain by summing the granular beta estimates defined in equation (6) over all the G partitions:

$$\hat{\beta}_{i,t} = \sum_{j=1}^{G} \widehat{\mathrm{G}\beta}_{i,t,j},$$

mirroring the previous discussion in Section 3.1 for the true latent betas.

3.3. Estimating the risk premium function

Our approach for estimating the risk premium function builds directly on the traditional Fama-MacBeth approach for estimating the risk premiums in linear factor pricing models. However, instead of regressing the returns on each of the assets on their factor loadings ("betas") to estimate the scalar risk premiums ("lambdas"), we instead regress the asset returns on the granular beta functions defined in equation (3). With a slight abuse of notation:

$$Y_{i,t} = \alpha_t + \int_{-\infty}^{\infty} \lambda_t(x) \mathrm{G}\beta^*_{i,t-1}(x) f_{X,t-1}(x) dx + e_{i,t}, \qquad i = 1, 2, ..., N. \tag{9}$$

This may formally be interpreted as a random field regression (Cohen and Jones, 1969), in which the scalar asset returns, $Y_{i,t}$, are regressed on the random functions, $\mathrm{G}\beta^*_{i,t-1}(\cdot)$. The output from this "regression" will in turn provide an estimate for the intercept parameter α_t, and the functional slope coefficient $\lambda_t(\cdot)$. That is, in contrast to the estimate for "lambda" obtained from the traditional Fama-MacBeth approach, which characterizes the average compensation for beta-related risk, the estimated lambda function from (9)

[4] In our empirical analyses discussed below, we rely on rolling windows of $S = 1,200$ trading days, or approximately five years, to estimate a given month's granular beta.

describes the compensation for systematic risk earned across the entire support of the underlying risk factor.

Mimicking the theoretical pricing equation in (4), the random field regression in (9) relies on the granular beta functions defined in (3) that obtain in the limit as the width of the partitions converge to zero. In practice, of course, with a finite number of return observations and without the imposition of any additional assumptions, we can only meaningfully estimate a finite number of granular betas. Correspondingly, we resort to the feasible estimates for the G granular betas defined in equations (6)-(8), together with the method of sieves (see Chen, 2007, for a review) to estimate the lambda function. Specifically:

$$\begin{aligned} Y_{i,t} &= \alpha_t + \sum_{j=1}^{G} \widehat{\mathrm{G}\beta}_{i,t-1,j} \lambda_t(j; G, p) + e_{i,t}, \\ &= \alpha_t + \sum_{j=1}^{G} \widehat{\mathrm{G}\beta}_{i,t-1,j} \mathbf{LP}(2j/G - 1, p) \boldsymbol{\phi}_t + e_{i,t}, \qquad i = 1, 2, ..., N, \end{aligned} \tag{10}$$

where $\boldsymbol{\phi}_t$ denotes the vector of coefficients to be estimated, and $\mathbf{LP}(x, p)$ refers to the deterministic $1 \times (p + 1)$-vector of Legendre polynomial transformations that we use for spanning the lambda function.[5] Consistent with economic intuition, the sieve approach also automatically ensures that the estimate for $\lambda_t(\cdot)$ defined by $\mathbf{LP}(2j/G - 1, p)\hat{\boldsymbol{\phi}}_t$ is smooth. As discussed further below, the use of a polynomial basis to span $\lambda_t(\cdot)$ also greatly facilitates the imposition and test of specific economic hypotheses, including "flatness" as implied by the CAPM and other traditional asset pricing models.

Given a value for p, the functional relationship in (10) may be easily estimated by OLS. Concretely, let $\mathbf{Y}_t$ denote the N_t-vector of returns, $\widehat{\mathrm{G}\beta}_{t-1}$ denote the $N_t \times G$ matrix of stacked granular betas, and $\mathrm{LP}(p)$ denote the $G \times (p + 1)$ matrix of polynomial

[5] Other polynomials, could, of course, be used as well as. However, the $2j/G - 1$ Legendre polynomial transformations that we rely on conveniently put the partitions on the [-1,1] interval. Unlike standard polynomial functions, the Legendre polynomials are also orthogonal on the [-1,1] interval with respect to the uniform distribution, so that regressions with high polynomial orders are less susceptible to multicollinearity; see also Li, Liao and Quaedvlieg (2022) for additional discussion and justification.

bases. Further define $\mathbf{Q}_t \equiv [\boldsymbol{\iota} \quad \mathrm{LP}(p)\widehat{\mathrm{G}\beta}_{t-1}]$, where $\boldsymbol{\iota}$ is a vector of ones. The parameter estimates are then simply obtained as:

$$[\hat{\alpha}_t \quad \hat{\boldsymbol{\phi}}_t]' = (\mathbf{Q}_t'\mathbf{Q}_t)^{-1}\mathbf{Q}_t'Y_t. \tag{11}$$

Moreover, standard errors robust to cross-sectional heteroskedasticity are easily obtained from the conventional Eicker-Huber-White covariance matrix:

$$Var([\hat{\alpha}_t \quad \hat{\boldsymbol{\phi}}_t]') = (\mathbf{Q}_t'\mathbf{Q}_t)^{-1}\mathbf{Q}_t' diag(\hat{\mathbf{e}}_t\hat{\mathbf{e}}_t')\mathbf{Q}_t(\mathbf{Q}_t'\mathbf{Q}_t)^{-1}, \tag{12}$$

where $\hat{\mathbf{e}}_t$ denotes the $N_t \times 1$ vector of residuals from equation (10). Inference concerning the estimated conditional lambda function also readily follows from the use of the delta method, and the fact that $\hat{\lambda}_t(j; G, p) = \mathbf{LP}(2j/G - 1, p)\hat{\boldsymbol{\phi}}_t$.

The theory of sieves formally requires that the polynomial order p grows to infinity together with the size of the estimation sample (see, e.g., Chen, 2007). In practice, of course, we will have to chose a specific value of p for the $\mathbf{LP}(x, p)$ polynomial. As discussed further in Section 4.2 below, in our empirical analyses we follow common practice in the literature and resort to cross-validation techniques for doing so. In addition to help mitigate possible over-fitting, we also introduce a second hyperparameter, ω. This additional regularization parameter serves to shrink the unrestricted $\hat{\lambda}_t(\cdot)$ estimates obtained for a given value of p towards the estimated "flat" lambda function obtained for $p \equiv 0$. Accordingly, our final estimate of $\lambda_t(\cdot)$ is constructed as:

$$\hat{\lambda}_t(j; G, p, \omega) = \omega\hat{\lambda}_t(j; G, 0) + (1 - \omega)\hat{\lambda}_t(j, G, p) \tag{13}$$

where $\omega = 0$ corresponds to no shrinkage, while for $\omega = 1$ the estimate is completely shrunk to a "flat" function. In parallel to our choice of p, in our empirical analyses we rely on standard cross-validation techniques for choosing the value of ω, as further discussed in Section 4.2 below.[6]

Analogous to the second-stage regression in the traditional Fama-MacBeth approach used for estimating the risk premiums in linear factor pricing models, all of the functional $\hat{\lambda}_t(\cdot)$ estimates discussed above pertain to a single time period t. In empirical applications, to help reduce the "noise" and more clearly delineate the economic implications, it is common to instead consider the average estimates obtained over the full sample, say $t = 1, 2, ..., T$. In the present context that is:

$$\hat{\lambda}(j; G, p, \omega) = \frac{1}{T} \sum_{t=1}^{T} \hat{\lambda}_t(j; G, p, \omega). \tag{14}$$

Following standard procedures, robust inference for these full-sample risk premium functions may also easily be obtain using an estimate of the long-run covariance matrix (e.g., Newey and West, 1987) for the time series of the individual lambda function estimates.

3.4. Testing economic restrictions

The sieve approach allows for the meaningful estimation of the risk premium function by succinctly parameterizing it using polynomial basis functions. As previously noted, the use of a polynomial bases to span the function also easily permits the imposition of various restrictions on the shape of the function.

Specifically, let $\phi_{t,i}$ denote the coefficient associated with the i^{th} polynomial basis function in period t, with $\phi_{t,1}$ denoting the linear coefficient, $\phi_{t,2}$ denoting the quadratic coefficient, etc. The "flatness" condition for the lambda function discussed in Section 3.1 above in connection with the implications of the traditional CAPM, corresponding to $\lambda(x) = \bar{\lambda}$ for all values of x, may then simply be imposed by fixing $\phi_{t,i} = 0$ for all i, except $i = 0$.

In a frictionless financial market, without any short-sale or leverage constraints, the lambda function would naturally also be symmetric around zero, as a short position in

[6]The granularity G may similarly be interpreted as a hyperparameter. However, rather than trying to select a single "optimal" value of G, we purposely present the estimates obtained across a range of values of G to explicitly illustrate the added flexibility afforded by larger values of G.

Y_i simply switches the sign of the granular beta function (see also the related discussion in Bollerslev et al., 2022b). Correspondingly, we will refer to lambda functions for which $\lambda(x) = \lambda(-x)$ as satisfying a "symmetry" condition in the sequel. Of course, legal constraints, higher costs association with short selling, and other impediments, may create limits-to-arbitrage and arbitrage risk (see, e.g., Pontiff, 1996; Schleifer and Vishny, 1997; Hong and Sraer, 2016), thereby causing $\lambda(x) \neq \lambda(-x)$.[7] Intuitively, if X is a market factor as in the CAPM, assets that covary more strongly with the market when the market is performing poorly tend to exacerbate downside risk, while assets that covary less with the market when the market is performing poorly help mitigate downside risk (Ang et al., 2006; Chabi-Yo et al., 2022). Accordingly, the latter type of assets may on average demand less of a risk premium causing the lambda function to be asymmetric. Just as for the flatness condition, this symmetry condition can also easily be imposed and tested by relying on partitions that are symmetric around zero and fixing $\phi_{t,i} = 0$ for all odd integers i (see Appendix B for additional details).

Meanwhile, when evaluating the full-sample lambda function estimates defined in (14), it is not possible to directly test for flatness or symmetry based on the ϕ_t parameters, as different combinations of the polynomial coefficients for the individually estimated $\hat{\lambda}_t(\cdot)$ functions may result in non-flat and/or asymmetric average lambda functions $\hat{\lambda}(\cdot)$, even when the average of the individually estimated parameters do not.[8] Thus, when considering hypotheses based on the full-sample lambda function estimates, we instead tests the hypotheses of interest by directly evaluating the average function estimates at B pre-set fixed points. That is, we test symmetry by:

$$H_0^{(Sym)} : \ \lambda^{(Unr)}(j; G, p, \omega) - \lambda^{(Sym)}(j; G, \tilde{p}, \tilde{\omega}) = 0, \quad \forall\ j = 1, ..., B, \tag{15}$$

[7] See also the recent discussion and extensive literature review in Gârleanu, Panageas and Zheng (2022) pertaining to the performance of shorting strategies and various economic constraints and mechanisms that might impede arbitrage.

[8] For example, when $p = 4$, similar functions can be obtained with $\phi_2 > 0,\ \phi_4 < 0$ and $\phi_2 < 0,\ \phi_4 > 0$, making it possible that the coefficients are zero on average, while in each single period, and therefore on average, the lambda function is non-flat.

and the stronger flatness condition by:

$$H_0^{(Flat)}:\ \lambda^{(Unr)}(j;G,p,\omega)-\lambda^{(Flat)}(j;G,0,0)=0,\quad \forall\ j=1,...,B, \tag{16}$$

where the corresponding unrestricted functional estimate, $\hat{\lambda}^{(Unr)}$, allow all polynomials in the period-by-period lambda functions to have non-zero coefficients, while the symmetric functional estimate, $\hat{\lambda}^{(Sym)}$, only allows even powers in the individually estimated functions to have non-zero coefficients, and the individual estimates underlying the flat function estimate, $\lambda^{(Flat)}$, only has an intercept.[9]

3.5. Granular multi-factor models

All of the estimates and hypothesis tests discussed above pertains to a one-factor setting and pricing model. The same general ideas and intuition readily extends to the estimation and tests of granular K-factor models.

Specifically, in a direct extension of the one-factor case, consider the situation in which the partitions for the k^{th} factor only depends on that same factor. Analogous to equation (7), the j^{th} granular realized covariance for the k^{th} factor may then similarly be defined as:

$$\widehat{\mathrm{GCov}}_{i,k,t,j}=\sum_{s=t-R+1}^{t}(Y_{i,s}-\bar{Y}_t)(X_{k,s}-\bar{X}_{t,k})\mathbf{1}\{X_{k,s}\in\mathcal{G}_j\}. \tag{17}$$

Stacking the K factors and the j^{th} granular covariances into the $(K\times 1)$ vectors $\mathbf{X}_t=[X_{1,t},...,X_{k,t}]'$ and $\widehat{\mathbf{GCov}}_{i,t,j}$, respectively, the multi-factor granular beta estimates are then simply constructed as:[10]

$$\widehat{\mathbf{G}\boldsymbol{\beta}}_{i,t,j}=\hat{\mathbf{V}}_{x,t}^{-1}\widehat{\mathbf{GCov}}_{i,t,j}, \tag{18}$$

[9] Since the symmetric and flat estimates may also use different hyperparameters from the unrestricted estimates, we further optimize these hyperparameters in a separate validation sample from that of the test sample.

[10] In parallel to the one-factor case, the granular betas also sum to the usual factor betas when weighted by the probability of each partition. Mirroring the discussion pertaining the CAPM, in a strict K-factor model with orthogonal factors, the granular beta functions are also parabolas, with proportionality coefficients equal to the factor loadings.

where

$$\hat{\mathbf{V}}_{x,t} = \sum_{s=t-R+1}^{t} (\mathbf{X}_s - \bar{\mathbf{X}}_t)(\mathbf{X}_s - \bar{\mathbf{X}}_t)'. \tag{19}$$

Replacing $\widehat{\mathrm{G}\beta}_{i,t-1,j}$ in the sieve regression defined in (10) above with $\widehat{\mathbf{G}\boldsymbol{\beta}}_{i,t,j}$, the joint estimation of the $\lambda_{k,t}(\cdot)$ risk premium functions for each of the K factors, together with inference and hypotheses testing, proceeds exactly as in the one-factor case.

With a total of G partitions for each of the factors, the specification discussed above results in a total of $K \times G$ granular betas. More involved multi-factor specifications in which the factors are jointly partitioned could, of course, be entertained as well. In an extension of our main empirical analysis, Section 5.2 briefly considers such a multi-dimensional approach. However, this extension comes at the expense of additional notational complexity, and we defer a more detailed discussion to that section. Instead, we turn next to a discussion of the data and estimation setup that we rely on throughout our empirical analyses.

4. Estimates of the risk premium function

4.1. Data

Our empirical analyses rely on daily return data from the Center for Research in Securities Prices (CRSP) database, spanning the period July 1963 to December 2020. Following standard practice, we consider all stocks with CRSP codes 10 and 11, and remove all "penny stocks" with prices less than five dollars to alleviate biases arising from price discreteness. We further require five years of daily data to estimate the granular betas, which leads to a total of 181,804 firm-month observations.

We focus our attention on the one-factor CAPM, the Fama and French (1992) three-factor model (FF3), the Carhart (1997) four-factor model (FF3+Mom), and the Fama and French (2015) five-factor model (FF5). These models have arguably emerged as the leading factor models in the literature. The returns for all of the factors, as well as the risk-free rate needed to compute the excess returns, are taken from Ken French's website.

As a reference, Appendix C reports the traditional annualized full-sample Fama-MacBeth risk premium estimates obtained for each of the models. We also report the estimates obtained by splitting each of the factors into separate up and down components.

4.2. Sample selection and tuning parameters

As discussed in Section 3.3, our use of a local polynomial approach for estimating the more advanced risk premium functions introduces two additional hyperparameters, p and ω. As noted in that same section, we rely on standard cross-validation techniques for choosing these parameters. This in turn also dictates our choice of estimation and forecasting samples.

Specifically, we begin by estimating the requisite granular beta functions using the $1,200$ daily returns up until the start of the month over which the monthly returns that we use in estimating the risk premium functions are measured. For a given ordering of the assets, we then use the first 60% of assets to estimate the α_t and $\boldsymbol{\phi}_t$ parameters in (10) on a month-by-month basis for a range of different values of the two hyperparameters. We then use the next 20% of assets as a validation sample to select the polynomial order and degree of shrinkage based on the average R^2 obtained for this collection of assets. Finally, we use the resulting estimated risk premium functions to price the remaining 20% of the assets. Accordingly, the results obtained for these remaining 20% of the stocks are an "out-of-sample" test of the estimated risk premium functions. Since the order of the assets is arbitrary, we repeat this procedure one hundred times for different random permutations of assets, and report the averages obtained across these permutations as our final estimation results.

4.3. Granular factor models

We commence our empirical analysis by considering a granular version of the standard CAPM. The resulting risk premium function estimates, $\hat{\lambda}(\cdot)$, are presented in Figure 2 as a function of the quantiles of the market return q_f (ranging from zero to one). To help illustrate the approach, we report the results obtained for different degrees of granularity,

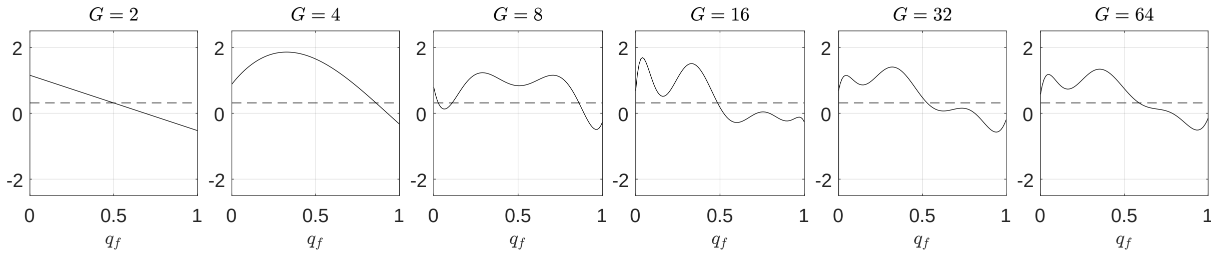

Figure 2: **Market factor risk premium function estimates.** The figure presents the estimated market risk premium function as a function of the market return quantiles for various functional beta granularities (G). The dashed lines report the standard Fama-Macbeth CAPM estimate obtained for $G = 1$.

increasing from $G = 1$, reported in all panels and corresponding to the traditional "flat" CAPM benchmark case, to $G = 2$ and all the way up to $G = 64$.

Looking at the $G = 2$ case, corresponding to the up- and down-side betas of Ang et al. (2006), confirms the finding that the market risk premium is larger when the market is down (i.e., for the left half of its support). As G increases, the estimated risk premium function is allowed to take more flexible shapes. However, by $G = 16$ the function has essentially converged, as there appears to be little systematic change in the shape when considering larger values of G. Broadly consistent with the up- and down-side CAPM, the risk premium function is generally positive when the market return is below its median, and close to zero when the market is above its median.

Extending these CAPM-based results, we next consider granular versions of the FF3, FF3+Mom, and FF5 models. To help streamline the presentation, we focus on the most flexible $G = 64$ granular beta models. Figure 3 presents the resulting estimated risk premium functions, along with 95% pointwise confidence intervals. The top-left panel in the figure corresponds directly to the right-most panel in Figure 2, with confidence intervals included.

The new results for the three-factor FF3 model given in the second row of Figure 3 show that the estimated market risk premium function remains qualitatively the same as in the CAPM model in the top row: the market risk premium is positive and significant when the market return is in its left tail, while not significantly different from zero for points in the support of the market return distribution slightly above its median. The fact that the estimated function appears smoother is attributable to the selected polynomial order for the market factor in the FF3 model being lower than in the CAPM, consistent with a greater need for parsimony in larger models.[11]

Turning to the other factors in the FF3 model, the risk premium function for SMB exhibits a U-shape. At the same time, however, the confidence intervals indicate that the function is not significantly different from being flat, a restriction that we formally test (and do not reject) below. Related, while the size effect was on average positive and significant up until around 1980 (Banz, 1981; Reinganum, 1981), the size risk premium, estimated using standard methods, has been found to be insignificant with more recent data (Schwert, 2003; Ahn, Min and Yoon, 2019).

The estimated risk premium function for HML evidence a more pronounced U-shape, with significant negative premiums when HML is around its median and significantly positive premiums for realizations in either of its tails. Consistent with many other studies documenting that the value premium has substantially weakened over the years, and perhaps even disappeared (e.g., Fama and French, 2020), the traditional full-sample Fama-Macbeth risk premium estimate for HML (reported in Appendix C), which effectively averages the lambda function over the support of the HML factor, is also not significantly different from zero. However, the more nuanced picture afforded by the functional estimate in Figure 3 tells a more complex story.

The third row of Figure 3 shows the estimation results for the FF3+Mom model. Not surprisingly, the estimated risk premium functions for the first three factors are all broadly in line with the results for the FF3 model, while the premium function for the momentum factor appears mildly non-linear. Finally, looking at the bottom row in Figure 3 and the estimates for the FF5 model, shows that the risk premium function for profitability (RMW) appears roughly flat. Meanwhile, the risk premium function for the investment (CMA) factor is almost the mirror image of the function for the market

[11] In particular, while the selected polynomial order for the CAPM is eight, in the FF3 it is only three. The cross-validated optimal polynomial and shrinkage parameters for all the models that we consider are reported in Table D.2 in Appendix D.

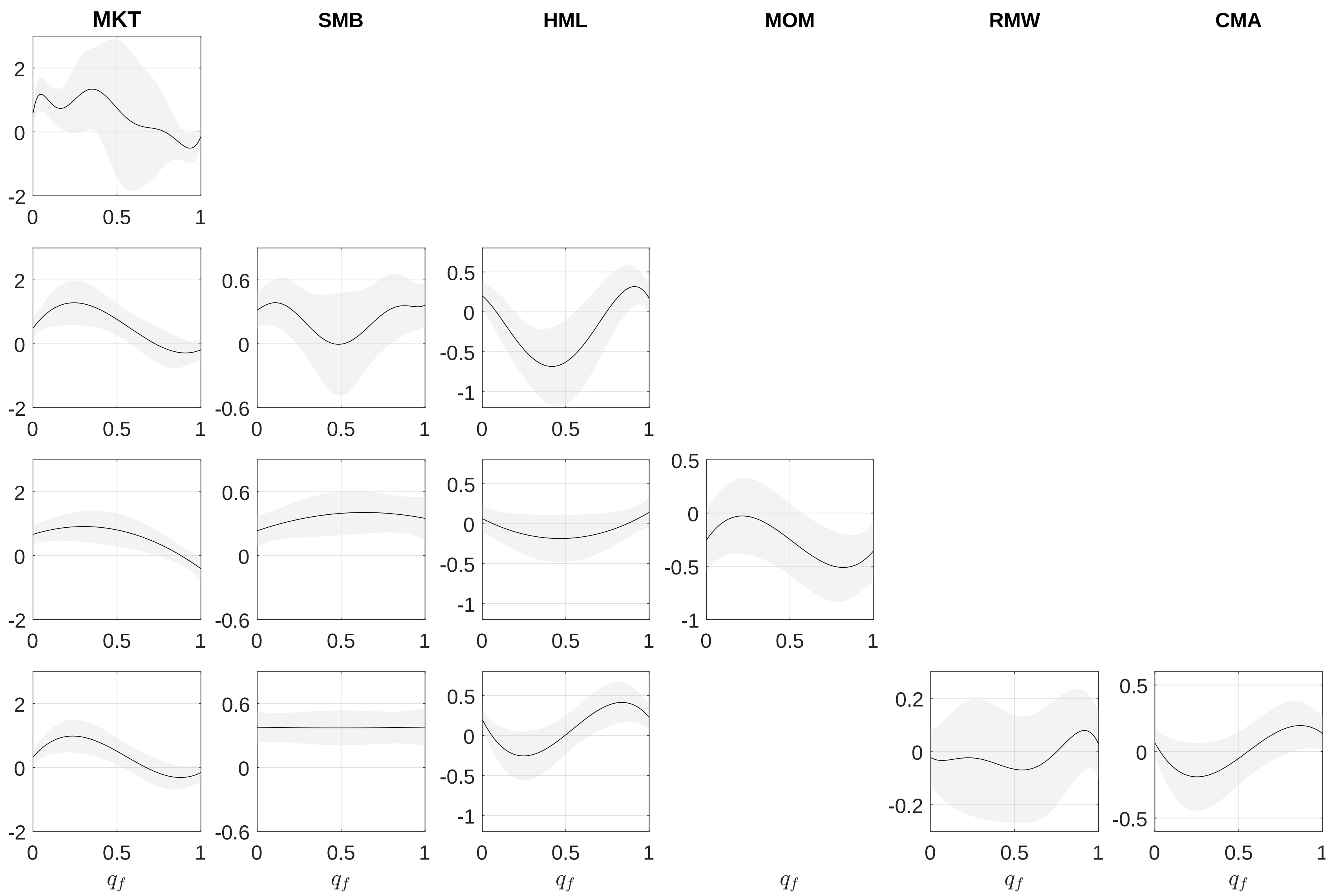

Figure 3: **Multi-factor risk premium function estimates.** The figure presents the estimated risk premium functions based on granular beta functions with $G = 64$, along with pointwise 95% robust confidence bounds. The rows correspond to the CAPM, FF3, FF3+Mom, and FF5 models, respectively.

factor: it is negative or zero for the left tail of the factor and earns a positive premium in the right tail.

In order to corroborate these visual impressions, Table 1 presents the results of our more formal tests for flatness and symmetry. We test the restrictions separately for each factor in a given model, as well as jointly across all factors in the model. In accord with the largest value of G used in the estimation of the granular beta functions, we rely on 64 equally-spaced points on the average (across time) estimated risk premium functions in implementing the tests, corresponding to $B = 64$ in equations (15) and (16).

Looking first at Panel A, which considers the null of symmetry as stipulated in (15), we observe that the p-values for the joint tests reported in the left-most column are all zero to three decimal places, indicating a strong rejection of the hypothesis. The tests for each of the factors individually, reported in columns two through seven, reveal that the strongest evidence against symmetry comes, perhaps not surprisingly, from the market factor, followed by the momentum and value factors. Tests of risk premium function symmetry for the remaining three factors, size, profitability, and investment, all fail to reject the null at conventional levels.

Panel B in turn tests the stronger restriction that the risk premium functions are flat, as stipulated by the null in (16). We again see that this restriction is strongly rejected for all of the models, with the p-values for the joint tests for the CAPM, FF3 and FF5 models all being less than one percent, and that for the FF3+Mom model being less than three percent.[12] In line with the previous tests of symmetry, these rejections are again predominantly driven by the estimates for the market, value, and momentum risk premium functions. Indeed, consistent with the visual impression from the estimates depicted in Figure 3, neither size, profitability nor investment exhibit any significant evidence against flatness.

[12] Since the hypothesis that the risk premium function is flat formally encompasses the hypothesis that the function is symmetric, one would naturally expect this hypothesis to be more strongly rejected by the data. However, random sampling variation can obviously result in more power to reject the specific null hypotheses stipulated in (15) compared to (16).

Table 1: **Tests on risk premium functions.** The table reports p-values from tests of the restrictions on the risk premium function in (15) and (16). The tests are implemented using 64 equally-spaced points on the average (across time) risk premium function estimates. Column 1 reports the results from joint tests for all of the factors in a given model, while columns 2-7 report the results from testing each of the factors individually.

	Joint	MKT	SMB	HML	MOM	RMW	CMA
Panel A. $H_0 : \lambda$ **is symmetric**							
CAPM	0.000	0.000					
FF3	0.000	0.000	1.000	0.089			
FF3+Mom	0.000	0.000	0.969	0.100	0.004		
FF5	0.000	0.000	0.983	0.000		0.231	0.156
Panel B. $H_0 : \lambda$ **is flat**							
CAPM	0.007	0.007					
FF3	0.000	0.000	1.000	0.000			
FF3+Mom	0.029	0.000	1.000	0.091	0.076		
FF5	0.000	0.000	1.000	0.000		1.000	0.114

Having established that the risk premium function estimates for the different factor models are generally statistically different from being simple flat lines, we next seek to assess the improvement, or lack thereof, in out-of-sample (OOS) fit afforded by the new more flexible granular models. Recall that we always estimate the model parameters and hyperparameters using the first 60% and 20% of assets respectively, leaving the remaining 20% of assets for OOS model evaluation. In addition, to alleviate any sensitivity to the specific assets that appear in the OOS sample, we re-do that same analysis one hundred times, randomly permuting the assets in each case.

Table 2 presents the resulting R^2 values averaged across the one hundred OOS permutations. To formally compare the benchmark (non-granular) factor models with their proposed granular counterparts, we use a Diebold and Mariano (1995) (DM) t-test to assess the significance, with positive values of the test statistics indicating that the granular models out-perform their non-granular benchmarks. However, since the one hundred

OOS permutations are correlated (some assets randomly appear in more than one test sample), we cannot simply average the DM test statistics as commonly done in the literature. Instead, as a (very) conservative approach, Table 2 reports the *minimum* DM test statistics obtained across all the one hundred permutations. As the table shows, when $G \geq 4$ the minimum DM test statistic is always at least two, indicating that the granular factor models provide significant improvements over their non-granular benchmarks.[13]

Examining the magnitudes of the R^2 values in Table 2, further reveals that the granular CAPM has an OOS R^2 that is roughly halfway between the non-granular CAPM and the non-granular FF3 model (3.8% compared with 3.1% and 4.4%, respectively), indicating that substantial gains in explanatory power can be achieved by using granular information, even without exploiting information from additional factors. Further corroborating that idea, the granular FF3 model also out-performs both of the non-granular FF3+Mom and FF5 models in terms of their OOS R^2s (5.3% compared with 5.2% and 5.0%, respectively). In other words, the results in Table 2 show that significant gains in predictive accuracy can be obtained from using the richer information in the new granular betas and associated risk premium functions.

To help appreciate where these forecast improvements are coming from, we next highlight how the granular models manifest in differences in the implied expected return functions for different types of assets.

4.4. Expected return functions

Even though the compensation for exposure to the different factor risks are obviously the same across assets, as explicated in equation (4) the variations in the magnitude and the shape of the granular beta functions, $\mathrm{G}\beta^*_{i,k}(\cdot)$, interact with the risk premium functions, $\lambda_k(\cdot)$, to generate differences in the "expected return functions" across assets. To illustrate, Figure 4 plots the expected return functions implied by the CAPM, FF3,

[13]For $G = 2$, the granular CAPM and FF5 models have minimum t-statistics of 1.6 and 1.7, respectively, suggesting only borderline significance. At the same time, however, the median t-statistics for these two models equal 3.3 and 5.3 respectively, corroborating that they too out-perform their benchmark non-granular counterparts.

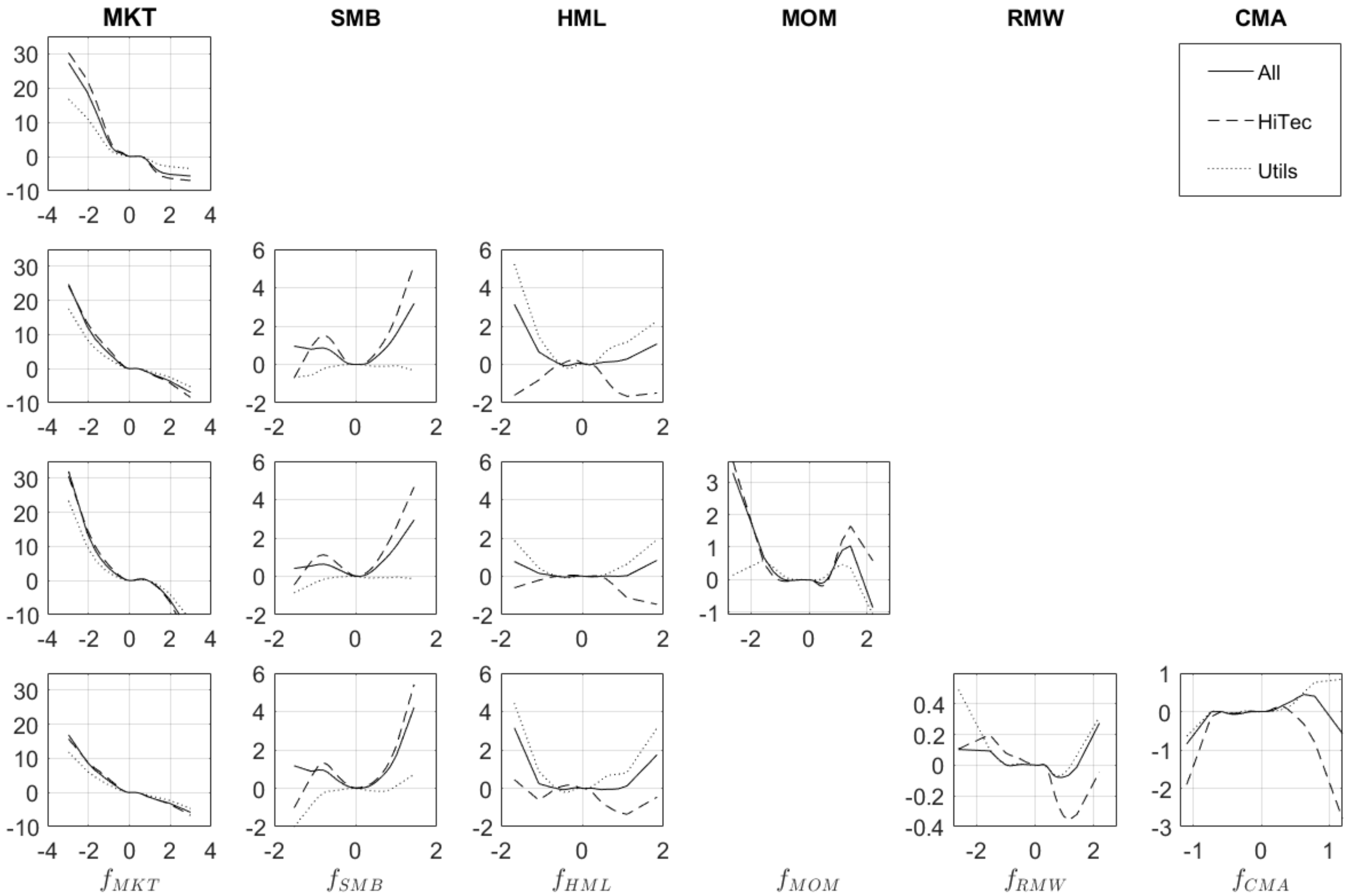

Figure 4: **Expected return functions.** The figure presents the expected return functions implied by the CAPM, FF3, FF3+Mom and FF5 granular models averaged across all of the stocks in the sample (All), together with portfolios comprised of technology stocks (HiTech) and utility stocks (Utils). The expected return functions are plotted as a function of the underlying factor returns.

Table 2: **Out-of-sample explanatory power.** The table presents the out-of-sample R^2s for the CAPM, FF3, FF3+Mom and FF5 factor models, estimated using standard OLS ($G = 1$) and granular betas with an increasing degree of granularity ($G > 1$). The reported values are averaged across the one hundred random cross-validation samples. The numbers in parentheses below the R^2s report the *minimum* Diebold and Mariano (1995) t-statistics across the one hundred random samples for testing whether the granular models out-perform their non-granular counterparts in the first row.

G	CAPM	FF3	FF3+Mom	FF5
1	3.145	4.447	5.204	5.040
2	3.484	4.966	5.622	5.337
	(1.557)	(2.383)	(2.470)	(1.673)
4	3.561	5.019	5.644	5.398
	(2.251)	(2.911)	(2.589)	(2.000)
8	3.693	5.143	5.692	5.466
	(3.016)	(3.449)	(3.111)	(2.275)
16	3.805	5.236	5.770	5.536
	(4.132)	(3.594)	(3.077)	(2.558)
32	3.795	5.282	5.785	5.559
	(3.080)	(3.765)	(2.650)	(2.733)
64	3.840	5.275	5.787	5.549
	(3.331)	(3.782)	(2.783)	(2.834)

FF3+Mom and FF5 granular models as a function of the underlying factor returns averaged across all of the stocks in our sample (All), together with the implied expected return functions for the portfolios of technology stocks (HiTech) and utility stocks (Utils) previously discussed in Figure 1 in the introduction.[14]

Looking first at the left most column, all three groups of stocks exhibit roughly similar average expected return functions in regards to the market factor, although the Utils curves appear slightly flatter than the other two curves, regardless of which other factors are included in the model. The pronounced steepness in the curves for especially low market returns, is consistent with the suggestion by Lu and Murray (2019) that the CAPM needs to be augmented with an additional factor to capture expected returns

[14]The Online Supplemental Appendix further details the expected returns for other industry portfolios, and how said returns may be attributed to the different factors in the CAPM, FF3, FF3+Mom and FF5 granular models.

observed during deep market declines, or bear markets.

Even though all three portfolios earn little or no return when HML is near its median, when the value factor is in its tails the expected returns on utility stocks and most other stocks are high, while the expected returns on high tech stocks are low. Meanwhile, high tech stocks generally earn higher returns when the momentum factor is in its left tail, as do most other stocks, while the expected returns on utility stocks are mostly unaffected by the momentum factor. Similarly, the expected return on utility stocks appear largely unaffected by the size factor, while high tech stocks tend to earn higher returns when the size factor is in the right tail of its distribution, as do most other stocks.

In sum, the expected return functions implied by the granular betas and estimated lambda functions clearly differ across different types of stocks. These differences go beyond traditional factor models that restrict the compensation for factor risk to be the same regardless of the realizations of the factors.

5. Extensions and applications

We begin our additional analyses reported in this section by investigating whether the estimated risk premium functions vary systematically with various financial economic indicators. We then consider the use of joint partitioning of the factor space within the context of a multi-factor model. We conclude the section by considering the practical use of the granular betas in the construction of a simple long-short portfolio strategy. For the sake of brevity, we focus our attention on the workhorse FF3 model throughout these additional analyses.

5.1. Variation in the risk premium functions

Our main empirical analysis and discussion in Section 4 pertain to the estimates of the risk premium functions obtained by averaging the monthly lambda function estimates over the full sample. This directly mirrors the traditional risk premium estimates commonly reported in the asset pricing literature, which are similarly averaged over longer time periods. However, risk premiums may be sensitive to economic conditions and the market's ability to bear risk (see, e.g., Cochrane, 2017). Any full-sample risk premium estimates obviously mask such dependencies.

To shed further light on this issue, we therefore estimate separate lambda functions by averaging the monthly estimates conditional on three commonly used financial economic indicators: the Chicago Board of Options Exchange's VIX volatility index, the Financial Uncertainty index of Jurado, Ludvigson and Ng (2015)), and the UP versus DOWN market indicator of Cooper, Gutierrez and Hameed (2004).[15] Specifically, for the first two measures, we estimate separate lambda functions for months when the measures are above or below their median values. For the binary UP measure, which equals unity for 88% of the months in the sample, we simply estimate separate lambda functions for its UP and DOWN states.[16]

Using the inference procedures discussed in Section 3.4, we can easily test whether these conditional lambda functions are indeed significantly different from one another. Figure 5 plots the estimated conditional lambda functions for which that null is rejected at the 5% significance level. When the test for identical conditional lambda functions do not reject, we instead plot the full-sample unconditional estimates previously shown in the second row in Figure 3.

As the first column in the figure shows, the risk premium function for the market factor varies significantly with both the Financial Uncertainty index and the UP/DOWN market indicator. In particular, consistent with the idea that the risk bearing capacity is lower when financial uncertainty is high and during down markets, the corresponding risk premium function estimates are both notably higher in those states compared to their low and up market counterparts. The overall shape of the estimated market risk

[15]We retrieve the VIX from the CBOE website. We use the Financial Uncertainty (one-month ahead) measure retrieved from `www.sydneyludvigson.com`. The UP measure equals one if the current market index price is higher than three years ago, and zero otherwise. We compute this index based on the market factor from Ken French's website.

[16]For comparison, the Online Supplemental Appendix also presents additional lambda function estimates obtained by splitting the full sample into shorter non-overlapping 20-year periods.

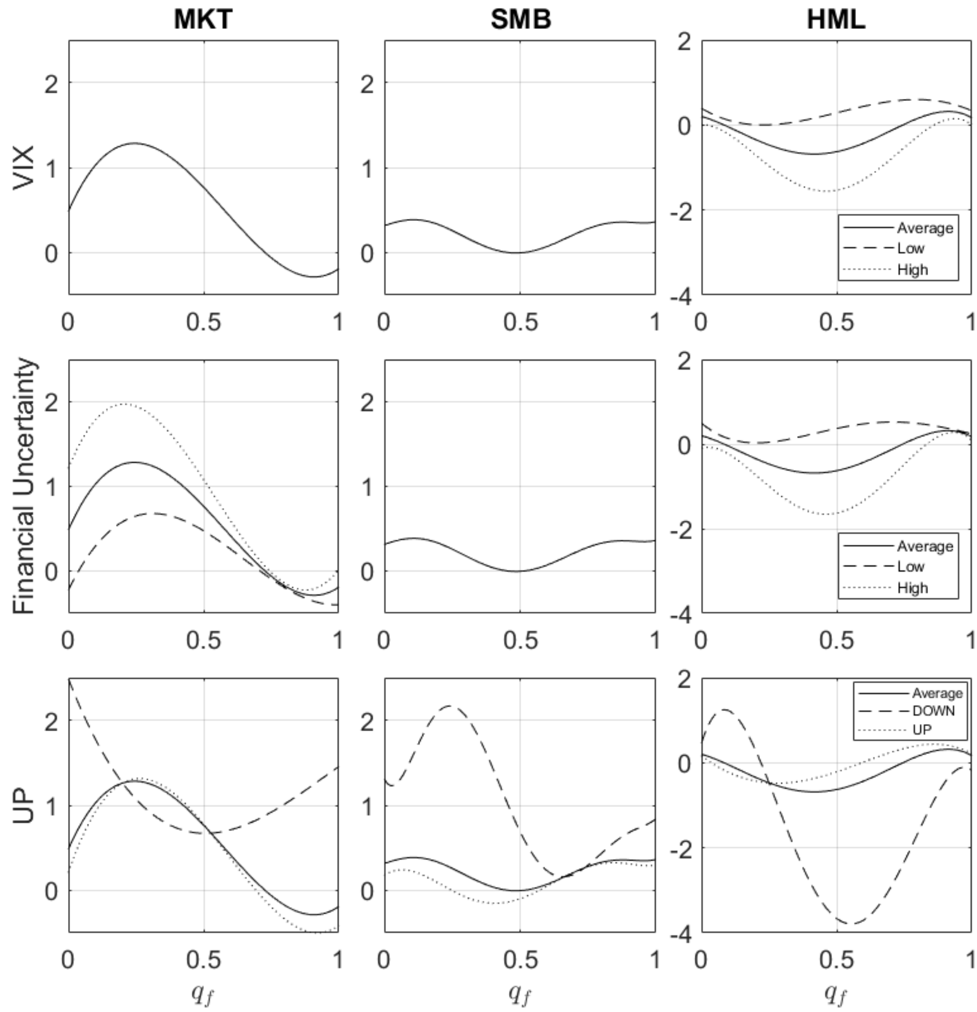

Figure 5: **Risk premium function estimates for different financial market conditions.** The figure presents the estimated risk premium functions for the FF3 model conditional on above and below median values of the VIX and the Financial Uncertainty index, as well as UP and DOWN market states. If the two estimated functions are not significantly different from one another at the 5% level, the figure plots the full-sample estimates.

premium functions seemingly also change between UP and DOWN markets, indicating that the high compensation for left tail risk documented in the literature is mostly earned during bear markets.

Looking at the results for the size factor in the second column of the figure, we see that while the estimated risk premium functions do not vary significantly with the VIX or the Financial Uncertainty index, they do differ between UP and DOWN markets. Indeed, it appears as if the size premium is primarily attributable to higher returns on small firms in DOWN markets. This more nuanced picture is also broadly consistent with Souza

(2020), who argues that the size premium is highly non-linear and mostly confined to "bad" economic states.

As previously noted, even though the HML premium as traditionally estimated is not significantly different from zero over the full sample, the estimated risk premium functions for the value factor differ significantly when conditioning on the state of each of the three financial economic indicators. In particular, while the estimated functions are fairly flat and close to zero when the VIX and Financial Uncertainty are low and the market is in its UP state, the functions become notably more curved in the high and DOWN states, with especially pronounced negative deviations from zero in the center of the distribution of the HML factor.

These conditional depictions of when and where the factor risk premiums are earned may help shed new light on predictability of the equity premium as it relates to the phases of the business cycle and various economic indicators (see, e.g., Adrian, Crump and Vogt, 2019; Moench and Stein, 2021). We will not pursue that line of questioning any further here, however, turning instead to a discussion of the use of more refined multi-dimensional partitions.

5.2. Multi-dimensional partitions

The granular betas considered so far all rely on partitions determined by a single factor at a time. In a K-factor model one might naturally consider more refined partitions based on all K factors jointly. Building on the notion of partial covariances (Bollerslev et al., 2022a), it would also be possible to condition the partitions on other variables in addition to the factor(s) actually included in the model. We now consider such extensions of our basic approach.

To set out the ideas, consider a K-factor model, where the support of each factor is partitioned into G regions. Denote the j^{th} partition of the k^{th} factor by $\mathcal{G}_j^k$. Considering all possible combinations of partitions across the K variables, $\mathcal{J} \equiv (j_1, j_2, ..., j_K) \in \{1, 2, ..., G\}^K$, we then end up with a total of $K \times G^K$ granular betas. By contrast, the previous one-dimensional partitions "only" generate $K \times G$ granular betas. In parallel to the estimates for the simpler one-dimensional case in (6) and (7), we obtain the multi-dimensional granular covariances and granular betas as:

$$\widehat{\text{GCov}}^{\mathcal{J}}_{i,t,k} = \sum_{s=t-R+1}^{t} (Y_{i,s} - \bar{Y}_t)(X_{k,s} - \bar{X}_{k,t}) \mathbf{1}\{\mathbf{X}_s \in \mathcal{G}^1_{j_1} \times \mathcal{G}^2_{j_2} \times \cdots \times \mathcal{G}^K_{j_K}\},$$

and

$$\widehat{\mathbf{G}\boldsymbol{\beta}}^{\mathcal{J}}_{i,t} = \hat{\mathbf{V}}^{-1}_{x,t} \widehat{\mathbf{GCov}}^{\mathcal{J}}_{i,t},$$

where $\widehat{\mathbf{GCov}}^{\mathcal{J}}_{i,t}$ denotes the $K \times 1$ vector of granular covariances across the K factors, for the $\mathcal{J}$ multi-dimensional partition. That is, we compute the covariance between the test asset, Y_i, and the k^{th} factor, X_k, conditioning on the first factor return lying in $\mathcal{G}^1_{j_1}$ and the second factor return lying in $\mathcal{G}^2_{j_2}$, and so on up to the K^{th} factor return lying in $\mathcal{G}^K_{j_K}$.

If the factors are strongly correlated and G^K is "too large," there may be partitions that have few or no observations. When a given partition has few observations the estimated granular betas will naturally be less precise, and their explanatory power for the cross-section of returns will be diminished.[17] Of course, if the factors are only weakly correlated, as is the case in our FF3-based empirical analysis, this is less of concern. Also, since we rely on out-of-sample returns to asses model performance across a range of values of G, if a given multi-dimensional partition simply leads to "too many" poorly estimated granular betas, this will be revealed empirically.[18]

Having estimated the multi-dimensional granular betas, mirroring the approach in Section 4.3, we then estimate risk premium functions for each of the granular betas based on sieve approximations. Specifically, we use K-dimensional polynomials of the type $P(\boldsymbol{x}, p) = x_1^a \times x_2^b \times ... \times x_K^k$, where the order $a + b + ... + k$ is again determined by cross-validation. Since the number of polynomials in the basis now increases much more

[17] This is akin to the problem arising in Bryzgalova et al. (2021) in the context of the construction of informative "test assets," or portfolios.

[18] As a case in point, we find that five-way partitions of the traditional CAPM betas based on the five FF5 factors are simply too "noisy" to be useful for out-of-sample forecasting; for additional details see the Online Supplemental Appendix.

Table 3: **One-way versus three-way partitions for granular betas.** This table presents a comparison of the out-of-sample R^2s for the CAPM and the FF3 models obtained using one-way (left panel) or three-way (right panel) partitions. The order of the polynomials (G) in each row are selected so that the total number of granular betas (#Gβ) is the same for the one-way and three-way partitions.

	One-way partitions			*Three-way partitions*		
#Gβ	G	Opt. order	R^2	G	Opt. order	R^2
Panel A: CAPM						
1	1	0	3.145	1	0	3.145
8	8	6	3.693	2	2,2,2	4.834
64	64	8	3.840	4	2,2,2	4.789
Panel B: FF3						
3	1	0	4.447	1	0	4.447
24	8	2,2,2	5.236	2	2,2,2	5.213
192	64	3,6,4	5.275	4	2,2,2	5.220

rapidly as a function of the order, we consider at most up to fourth-order polynomials. We further restrict our attention to three-dimensional partitions, in which we partition the betas according to the market, size and value factors. To make the results based on the three-way partitions directly comparable to the previous results based on one-way partitions, we select the order G in each case so that the total number of granular betas on the right-hand side of the functional regressions are the same.[19]

Looking first at Panel A in Table 3 and the reference results for the CAPM, we see that the out-of-sample R^2, which as previously reported in Table 2 increases from 3.1% to 3.8% when allowing for one-way partitions, further increases to 4.8% when we allow for three-way partitions based on the FF3 factors. In other words, by more finely measuring the local covariation with the market, we greatly improve on the ability of the CAPM-based model to explain the cross-sectional variation in the returns. Of course, a more direct approach would be to simply include the two additional factors and work directly

[19] Recall that G one-way partitions of K factors leads to $K \times G$ granular betas, while K-way partitions leads to $K \times G^K$ granular betas.

with the FF3 three-factor model.

Meanwhile, we already know from our previous results that the FF3 model can be improved by considering one-dimensional partitions, with the R^2 increasing from 4.4% to 5.3%. In contrast to the results for the CAPM, however, looking at the new results for the FF3 model in Panel B in Table 3, there appears to be no additional gains available by allowing for three-dimensional partitions; in fact the R^2s decease just slightly.

In sum, while the simple one-factor CAPM can be improved by considering multi-dimensional granular betas based on the market, size and value factors, for larger multi-factor models the additional estimation error associated with multi-dimensional partitions seem to outweigh the gains, so that for multi-factor models the simpler granular betas based on one-dimensional partitions generally result in the best performing models.[20]

5.3. Long-short granular beta portfolios

To further underscore the practical value of the granular betas, we now consider a set of simple granular long-short portfolio strategies. Putting the new strategies into perspective, arguably the oldest of all factor related anomalies, dating back to Black, Jensen and Scholes (1972), holds that the empirical relationship between conventional market betas and returns is "too flat" to be explained by the standard CAPM. Accordingly, portfolios that "bet against beta" by going long in high-beta stocks, and short in low-beta stocks, tend to earn positive alphas (see, also Frazzini and Pedersen, 2014). In the granular beta setting, however, stock selection cannot simply depend on the risk exposures, but must also take into account the differences in the premiums earned for the different granular risk exposures. Hence, rather than simply sorting the stocks based on their granular betas, we instead sort the stocks based on their predicted expected returns implied by the granular betas and the corresponding estimated risk premium functions.

In particular, averaging across the expected return functions for each of the factors,

[20]These same conclusions are also corroborated by the additional empirical results for the FF3+Mom and FF5 factor models reported in the Online Supplemental Appendix.

we calculate the expected return for month t and stock i as:

$$\sum_{k=1}^{K}\sum_{j=1}^{G}\widehat{G\beta}_{t-60:t-1,i,k,j}\hat{\lambda}_{t-60:t-1}(j,G),$$

where we rely on a 60-month moving average for both the betas and the risk premium functions. For the sake of brevity, we again focus on the FF3 model, corresponding to $K = 3$. In addition to the expected return predictions from the full model, we also consider portfolios based on the expected return predictions stemming from each of the three individual factors at a time. Specifically, for stock i and factor k:

$$\sum_{j=1}^{G}\widehat{G\beta}_{t-60:t-1,i,k,j}\hat{\lambda}_{t-60:t-1}(j,G),$$

where we continue to rely on the lambda functions estimated for the full FF3 model.

Armed with the estimated expected returns for each of the stocks and months in the sample, we then construct long-short portfolios, in which the long leg consists of an equal-weighted portfolio of the 20% of the stocks with the highest expected returns for a given month, and the short-leg consists of an equal-weighted portfolio of the 20% of the stocks with the lowest monthly expected returns.[21] We consider $G = 1, 2$ and 64, representing the traditional FF3 model, the up- and downside version of the FF3 model, as well as the most flexible granular version of the FF3 model considered above.

The resulting portfolio performance is summarized in Table 4. Panel A reports the annualized mean and standard deviation of the portfolio returns, along with their Sharpe ratios. We also report the t-statistics for testing whether the Sharpe ratios for the granular-based portfolios are significantly higher than their $G = 1$ counterparts based on the test of Ledoit and Wolf (2008). Panel B in turn provides the corresponding alphas for each of the portfolios with respect to the traditional CAPM and the linear FF3, FF3+Mom and FF5 benchmark models, together with Newey-West robust t-statistics in

[21]For $G = 1$ and a single factor equal to the market, this naturally reduces to a simple "betting on beta" type portfolio.

Table 4: **Long-short granular beta portfolios** The top panel reports annualized descriptive statistics for long-short granular strategies. The columns marked MKT, HML and SMB, refer to portfolios based on a single factor, while the column marked Joint account for exposures to all three factors jointly. All of the portfolios are self-financing and rebalanced monthly based on a long-position in the 20% of stocks with the highest expected returns, and a short-position in the 20% of stocks with the lowest expected returns. The bottom panel reports the intercept and Newey-West robust t-statistics of time-series regressions for the standard CAPM, FF3, FF3+Mom and FF5 benchmark models. The alphas are reported in annualized percentage terms.

	MKT			SMB			HML			Joint		
G	1	2	64	1	2	64	1	2	64	1	2	64
Panel A: Descriptives												
Mean	0.601	2.831	3.898	1.972	2.725	3.324	0.133	0.103	1.022	2.669	2.862	3.909
StDev	15.81	15.06	14.48	11.41	11.69	12.06	11.32	11.15	11.99	13.95	13.99	13.98
Sharpe	0.038	0.188	0.269	0.173	0.233	0.276	0.012	0.009	0.085	0.191	0.205	0.280
t-stat		(1.927)	(2.923)		(1.927)	(2.110)		(-0.110)	(2.189)		(0.450)	(2.167)
Panel B: Alphas												
CAPM	-0.394	1.671	2.766	1.111	2.073	2.527	0.723	0.224	1.636	1.499	1.718	2.784
t-stat	(-0.346)	(1.549)	(2.674)	(1.426)	(2.574)	(3.016)	(0.874)	(0.274)	(1.856)	(1.472)	(1.659)	(2.408)
FF3	0.651	2.850	3.953	0.046	0.890	1.162	0.518	0.049	1.123	1.245	1.629	2.638
t-stat	(0.576)	(2.636)	(3.830)	(0.060)	(1.141)	(1.435)	(0.580)	(0.056)	(1.222)	(1.157)	(1.505)	(2.281)
FF3+Mom	1.440	3.825	4.668	-0.128	0.710	1.243	1.530	1.272	2.504	3.323	3.571	4.678
t-stat	(1.286)	(3.638)	(4.593)	(-0.163)	(0.891)	(1.525)	(1.722)	(1.450)	(2.728)	(3.222)	(3.405)	(4.331)
FF5	-0.218	1.839	3.229	-0.514	0.742	1.225	0.285	-0.258	1.042	1.356	1.812	2.715
t-stat	(-0.169)	(1.466)	(2.767)	(-0.642)	(0.874)	(1.431)	(0.304)	(-0.278)	(1.063)	(1.172)	(1.491)	(2.119)

parentheses.

As the table shows, the granular beta-based portfolio generally result in significantly higher Sharpe ratios. Since the portfolios are explicitly constructed to generate higher returns, the higher Sharpe ratios are almost exclusively driven by higher mean returns. The overall highest average realized returns and Sharpe ratio are, not surprisingly, achieved by the joint FF3 granular specification that utilizes the granular betas and risk premium functions for all three factors to jointly predict the expected returns. Looking at the results for each of the individual factors, illustrate that stock selection based on the granular betas and expected return function estimates for the MKT factor offer the largest (relative) single-factor improvements, followed by the SMB factor. This is also consistent with the visual impression from the earlier Figure 3 and the corresponding tests in Table 1 indicating that the market risk premium function is the furthest from being "flat."

These findings are corroborated by the alpha estimates reported in Panel B. For the $G = 1$ portfolios based on the standard linear models and factors, only a single of the sixteen different alphas is significant at the usual 5% level. This, of course, is not surprising as the standard portfolios are formed based on the same factors used in the benchmark models. Meanwhile, consistent with the differential pricing of up- and down-side market risk, the $G = 2$ portfolios based solely on the MKT factor do result in significant alphas with respect to the FF3 and FF3-Mom benchmark models. However, going one step further and more fully exploiting the granular information and potentially "hidden" compensation not captured by the traditional linear factor models, the $G = 64$ Joint and MKT-based portfolios result in significant positive alphas with respect to *all* of the traditional benchmark models.

6. Conclusion

Linear factor models remain the workhorse for understanding risk exposures and risk premiums in financial markets. In such models, risk exposures are traditionally measured using simple covariances, or betas, with respect to a given set of factors, with the risk premiums estimated as linear functions of these exposures. Instead, we propose a new approach for boosting the information that can be extracted from existing factors, without the need for any additional data. Drawing on earlier work emphasizing the differential pricing of up- and down-side betas, we propose and estimate new local measures of dependence. These new measures, which we dub "granular betas," allow for more refined characterizations of the intrinsic dependencies between an asset and a risk factor. We further exploit the cross-sectional variation in the resulting "granular beta functions" to estimate new "risk premium functions." These functional estimates generalize the scalar risk premium estimates from standard factor models and methods, and importantly allow us to precise where, in the support of the factor space, risk premiums are truly earned. Implementing the new procedures with a large cross-section of individual U.S. equity returns, we find that the fit of traditional factor models can be significantly improved by using our new more flexible "granular" approach.

Our new approach opens up many other empirical and theoretical questions. For instance, the more nuanced depiction of risk exposures provided by the granular betas suggests the opportunity for improved risk management practices by more precisely targeting specific factor risks. Related, new and "smarter beta" investment strategies geared toward specific parts of the factor space may also be possible. Our strong empirical evidence against flatness and symmetry for some of the factor risk premium functions also naturally raises the question of what are the economic mechanisms that drive these differences in compensation? We leave the answer to all of these tantalizing questions for future research.

Appendix A. The risk premium function under the CAPM

As discussed in Section 3.1, if the CAPM holds and expected returns satisfy $\mathbb{E}[Y_{i,t}|X_t] = \beta_i X_t$, the granular beta function must be a parabola, as defined in equation (5). To consider the risk premium function under the CAPM, it is helpful to decompose the function into a "flat" term, and a term that captures deviations from "flatness," say $\lambda(x) = \mu_x + \ddot{\lambda}(x)$. Equating the expected return on asset i under the CAPM, $\mu_i = \beta_i \mu_x$, with that implied by our random field regression, and substituting in the expression for $\mathrm{G}\beta_i$ then yields:

$$\begin{aligned}
\mu_i &= \alpha + \mathbb{E}[\lambda(X)\mathrm{G}\beta_i^*(X)] \\
&= \alpha + \mu_x \mathbb{E}[\mathrm{G}\beta_i^*(X)] + \mathbb{E}[\ddot{\lambda}(X)\mathrm{G}\beta_i^*(X)] \\
&= \alpha + \beta_i \mu_x + \beta_i \mathbb{E}\left[\ddot{\lambda}(X)\left(\frac{X-\mu_x}{\sigma_x}\right)^2\right], \qquad \text{(A.1)}
\end{aligned}$$

where the third line uses the fact that $\mathbb{E}[\mathrm{G}\beta_i^*(X)] = \beta_i$ and the functional form for $\mathrm{G}\beta_i^*(x)$ given in equation (5). Considering a zero-beta asset, it readily follows that $\alpha = 0$. Further, under the CAPM we have $\mu_i = \beta_i \mu_x \ \forall \ i$, and so the third term in equation (A.1) must equal zero for all i. Since β_i may differ from zero, the $\mathbb{E}[\cdot]$ term must therefore be identically equal to zero. Since the squared standardized market return is weakly positive, this can only hold if $\ddot{\lambda}(x) = 0 \ \forall \ x$. In other words, under the CAPM, the intercept in the regression, α, must be zero, and the lambda function must be flat, and equal to the expected return on the market for all x, that is, $\lambda(x) = \mu_x \ \forall \ x$.

Appendix B. Symmetrized quantiles

For simple parameter restrictions on the Legendre polynomial terms to be sufficient to imply symmetry, we need to use partition boundaries that are symmetric around zero. If the distributions of the factor returns were known to be symmetric, then we could simply use quantiles of these returns. If, however, the factor returns are asymmetrically distributed, as is the case in our empirical analysis, then an alternative set of boundaries are needed. Let $G > 1$ denote the number of desired partitions, and assume that G is even, as is the case in our empirical analysis. Let $H \equiv G/2$. We then use the quantiles of the absolute factor returns, defined by $\tilde{q}_\tau = Q^\tau[|X_t|]$ for $\tau = 1/H,\ 2/H,\ ...,\ (H-1)/H$. Accordingly, the $G-1$ partition boundaries are: $\left[-\tilde{q}_{(H-1)/H}, ..., -\tilde{q}_{1/H}, 0, \tilde{q}_{1/H}, \tilde{q}_{(H-1)/H}\right]$.

Appendix C. Traditional risk premium estimates

Table C.1: **Annualized Fama-Macbeth risk premium estimates.** The table reports the annualized risk premium estimates obtained for the traditional CAPM, FF3, FF3+Mom and FF5 models over the full sample (denoted G=1 in the table), along with the corresponding estimates for the up and down versions of the models (denoted G=2 in the table). Robust t-statistics are reported in parentheses.

	G = 1					G = 2			
	CAPM	FF3	FF3+Mom	FF5		CAPM	FF3	FF3+Mom	FF5
MKT	3.765	3.039	3.068	1.940	MKT^-	26.662	16.583	25.934	15.194
	(1.531)	(1.312)	(1.327)	(0.845)		(2.932)	(1.757)	(2.306)	(1.577)
					MKT^+	-19.167	-9.267	-20.208	-8.613
						(-2.417)	-(0.900)	(-1.703)	(-0.814)
SMB		4.249	3.829	4.621	SMB^-		6.415	3.362	6.575
		(3.227)	(3.119)	(3.568)			(1.288)	(0.672)	(1.195)
					SMB^+		0.821	2.502	1.113
							(0.143)	(0.403)	(0.179)
HML		1.515	0.313	1.865	HML^-		5.285	2.735	3.773
		(1.050)	(0.238)	(1.329)			(1.016)	(0.469)	(0.699)
					HML^+		-2.021	-1.163	0.587
							(-0.389)	(-0.190)	(0.099)
MOM			-3.226		MOM^-			-6.333	
			(-1.248)					(-0.792)	
					MOM^+			-4.601	
								(-0.628)	
RMW				0.148	RMW^-				-2.409
				(0.127)					(-0.669)
					RMW^+				3.380
									(0.863)
CMA				0.701	CMA^-				0.789
				(0.569)					(0.192)
					CMA^+				1.925
									(0.437)
Constant	6.673	6.030	5.878	7.207	Constant	6.375	5.680	5.721	6.020
	(2.889)	(2.873)	(2.782)	(3.235)		(2.798)	(2.722)	(2.704)	(2.659)

Appendix D. Hyperparameters

Table D.2: **Hyperparameter selection.** The table reports the polynomial orders used for estimating the risk premium functions for the different models, together with the shrinkage intensities towards the flat estimates ($G = 1$). The hyperparameters were determined by 60/20/20 cross-validation, as discussed in the main text.

G	Unrestricted	Functional						
		Order						
	ω	MKT	SMB	HML	MOM	RMW	CMA	ω
				CAPM				
1	0.28	0						0.63
2	0.57	1						0.56
4	0.70	3						0.70
8	0.76	6						0.75
16	0.82	8						0.76
32	0.86	8						0.76
64	0.93	8						0.75
				FF3				
1	0.04	0	0	0				0.10
2	0.66	1	1	1				0.66
4	0.78	3	2	3				0.77
8	0.85	2	2	2				0.71
16	0.91	3	4	4				0.76
32	0.97	3	6	4				0.78
64		3	6	4				0.78
				FF3+Mom				
1	0.07	0	0	0	0			0.20
2	0.72	1	1	1	1			0.72
4	0.83	3	2	3	2			0.82
8	0.89	3	2	2	2			0.80
16	0.94	6	4	3	3			0.82
32		3	6	4	3			0.82
64		2	2	2	3			0.78
				FF5				
1	0.02	0	0	0		0	0	0.10
2	0.78	1	1	1		0	0	0.72
4	0.86	3	2	3		2	2	0.84
8		2	4	6		2	4	0.86
16		6	2	4		5	5	0.86
32		3	2	3		5	4	0.84
64		3	2	3		5	4	0.84

References

Adrian, T., Crump, R.K., Vogt, E., 2019. Nonlinearity and flight-to-safety in the risk-return trade-off for stocks and bonds. Journal of Finance 74, 1931–1973.

Ahn, D.H., Min, B.K., Yoon, B., 2019. Why has the size effect disappeared? Journal of Banking and Finance 102, 256–276.

Aït-Sahalia, Y., Jacod, J., Xiu, D., 2021. Inference of risk premia in continuous-time asset pricing models. Working paper, Princeton University .

Aleti, S., 2022. The high-frequency factor zoo. Working paper, Duke University .

Andersen, T.G., Bollerslev, T., Diebold, F.X., Wu, G., 2006. Realized beta: Persistence and predictability, in: Fomby, T.B., Terrell, D. (Eds.), Advances in Econometrics: Econometric Analysis of Economic and Financial Time Series. Elsevier Science, Amsterdam. volume 20, pp. 1–40.

Andrews, D.W., 1991. Asymptotic normality of series estimators for nonparametric and semiparametric regression models. Econometrica , 307–345.

Ang, A., Chen, J., Xing, Y., 2006. Downside risk. Review of Financial Studies 19, 1191–1239.

Bali, T.G., Goyal, A., Huang, D., Jiang, F., 2022. Predicting corporate bond returns: Merton meets machine learning. Working paper, Georgetown University .

Banz, R.W., 1981. The relationship between return and market value of common stocks. Journal of Financial Economics 9, 3–18.

Barndorff-Nielsen, O.E., Kinnebrock, S., Shephard, N., 2010. Measuring downside risk: Realised semivariance, in: Bollerslev, T., Russell, J.R., Watson, M.W. (Eds.), Volatility and Time Series Econometrics: Essays in Honor of Robert F. Engle. Oxford University Press, Oxford, pp. 117–136.

Barndorff-Nielsen, O.E., Shephard, N., 2004. Econometric analysis of realized covariation: High frequency based covariance, regression, and correlation in financial economics. Econometrica 72, 885–925.

Baruník, J., Nevrla, M., 2020. Tail risks, investment horizons, and asset prices. Working Paper, Charles University, Czech Republic .

Beason, T., Schreindorfer, D., 2022. Dissecting the equity premium. Journal of Political Economy 130, 2203–2222.

Bianchi, D., Büchner, M., Tamoni, A., 2021. Bond risk premiums with machine learning. Review of Financial Studies 34, 1046–1089.

Black, F., Jensen, M., Scholes, M., 1972. The capital asset pricing model: Some empirical tests, in: Jensen, M. (Ed.), Studies in the Theory of Capital Markets. Praeger, New York, pp. 79–121.

Bollerslev, T., Li, J., Patton, A.J., Quaedvlieg, R., 2020. Realized semicovariances. Econometrica 88, 1515–1551.

Bollerslev, T., Li, S.Z., Todorov, V., 2016. Roughing up beta: Continuous versus discontinuous betas and the cross section of expected stock returns. Journal of Financial Economics 120, 464–490.

Bollerslev, T., Medeiros, M.C., Patton, A.J., Quaedvlieg, R., 2022a. From zero to hero: Realized partial (co)variances. forthcoming, Journal of Econometrics .

Bollerslev, T., Patton, A.J., Quaedvlieg, R., 2022b. Realized semibetas: Disentangling "good" and "bad" downside risks. Journal of Financial Economics 144, 227–246.

Bollerslev, T., Todorov, V., 2011. Tails, fears, and risk premia. Journal of Finance 66, 2165–2211.

Bryzgalova, S., Pelger, M., Zhu, J., 2021. Forest through the trees: Building cross-sections of stock returns. Working paper, London Business School .

Cai, Z., Fang, Y., Xu, Q., 2022. Testing capital asset pricing models using functional-coefficient panel data models with cross-sectional dependence. Journal of Econometrics 227, 114–133.

Carhart, M.M., 1997. On persistence in mutual fund performance. Journal of Finance 52, 57–82.

Chabi-Yo, F., Huggenberger, M., Weigert, F., 2022. Multivariate crash risk. Journal of Financial Economics 145, 129–153.

Chen, X., 2007. Large sample sieve estimation of semi-nonparametric models, in: Heckman, J., Leamer, E. (Eds.), Handbook of Econometrics. 1 ed.. Elsevier. volume 6B. chapter 76.

Cochrane, J., 2017. Macro-finance. Review of Finance 21, 945–985.

Cochrane, J.H., 2011. Presidential address: Discount rate. Journal of Finance 66, 1047–1108.

Cohen, A., Jones, R.H., 1969. Regression on a random field. Journal of the American Statistical Association 64, 1172–1182.

Cong, L.W., Feng, G., He, J., He, X., 2022. Asset pricing with panel tree under global split criteria. Working paper, Cornell University .

Conrad, J., Dittmar, R.F., Ghysels, E., 2013. Ex ante skewness and expected stock returns. Journal of Finance 68, 85–124.

Cooper, M.J., Gutierrez, Jr., R.C., Hameed, A., 2004. Market states and momentum. Journal of Finance 59, 1345–1365.

Diebold, F.X., Mariano, R.S., 1995. Comparing predictive accuracy. Journal of Business and Economic Statistics 13, 253–265.

Dittmar, R.F., 2002. Nonlinear pricing kernels, kurtosis preference, and evidence from the cross section of equity returns. Journal of Finance 57, 369–403.

Fama, E.F., French, K.R., 1992. The cross-section of expected stock returns. Journal of Finance 47, 427–465.

Fama, E.F., French, K.R., 2015. A five-factor asset pricing model. Journal of Financial Economics 116, 1–22.

Fama, E.F., French, K.R., 2020. The value premium. Working paper, University of Chicago .

Fan, J., Ke, Z., Liao, Y., Neuhierl, A., 2022. Structural deep learning in conditional asset pricing. Working paper, Princeton University .

Farago, A., Tedongap, R., 2018. Downside risks and the cross-section of asset returns. Journal of Financial Economics 129, 69–86.

Frazzini, A., Pedersen, L.H., 2014. Betting against beta. Journal of Financial Economics 111, 1–25.

Freyberger, J., Neuhierl, A., Weber, M., 2020. Dissecting characteristics nonparametrically. Review of Financial Studies 33, 2326–2377.

Gârleanu, N., Panageas, S., Zheng, G., 2022. A long and a short leg make for a wobbly equilibrium. Working paper, Washington University in St.Louis .

Gu, S., Kelly, B., Xiu, D., 2020. Empirical asset pricing via machine learning. Review of Financial Studies 33, 2223–2273.

Gul, F., 1991. A theory of disappointment aversion. Econometrica 59, 667–686.

Harvey, C.R., Siddique, A., 2000. Conditional skewness in asset pricing tests. Journal of Finance 55, 1263–1295.

Hong, H., Sraer, D.A., 2016. Speculative betas. Journal of Finance 71, 2095–2144.

Jurado, K., Ludvigson, S.C., Ng, S., 2015. Measuring uncertainty. American Economic Review 105, 1177–1216.

Kahneman, D., Tversky, A., 1979. Prospect theory: An analysis of decision under risk. Econometrica 47, 263–291.

Kelly, B., Jiang, H., 2014. Tail risk and asset prices. Review of Financial Studies 27, 2841–2871.

Kimball, M., 1993. Standard risk aversion. Econometrica 64, 589–611.

Kozak, S., Nagel, S., Santosh, S., 2020. Shrinking the cross section. Journal of Financial Economics 135, 271–292.

Langlois, H., 2020. Measuring skewness premia. Journal of Financial Economics 135, 399–424.

Ledoit, O., Wolf, M., 2008. Robust performance hypothesis testing with the sharpe ratio. Journal of Empirical Finance 15, 850–859.

Levi, Y., Welch, I., 2020. Symmetric and asymmetric market betas and downside risk.

Review of Financial Studies 33, 2772–2795.

Li, B., Rossi, A., 2022. Selecting mutual funds from the stocks they hold: A machne learning approach. Working paper, Georgetown University .

Li, J., Liao, Z., Quaedvlieg, R., 2022. Conditional superior predictive ability. Review of Economic Studies 89, 843–875.

Lintner, J., 1965. The valuation of risk assets and the selection of risky investments in stock portfolios and capital budgets. Review of Economics and Statistics 47, 13–37.

Lu, Z., Murray, S., 2019. Bear beta. Journal of Financial Economics 131, 736–760.

Massacci, D., Sarno, L., Trapani, L., 2021. Factor models with downside risk. Working paper, Kingâs College London .

Moench, E., Stein, T., 2021. Equity premium predictability over the business cycle. Working paper, Frankfurt School of Finance and Management .

Newey, W.K., 1997. Convergence rates and asymptotic normality for series estimators. Journal of Econometrics 79, 147–168.

Newey, W.K., West, K.D., 1987. A simple, positive semi-definite, heteroskedasticity and autocorrelation consistent covariance matrix. Econometrica 55, 703–708.

Patton, A.J., Sheppard, K., 2015. Good volatility, bad volatility: Signed jumps and the persistence of volatility. Review of Economics and Statistics 97, 683–397.

Patton, A.J., Verardo, M., 2012. Does beta move with news? Firm-specific information flows and learning about profitability. Review of Financial Studies 25, 2789–2839.

Pontiff, J., 1996. Costly arbitrage: Evidence from closed-end funds. Quarterly Journal of Economics 111, 1135–1151.

Reinganum, M.R., 1981. Misspecification of asset pricing: Empirical anomalies based on earnings yields and market values. Journal of Financial Economics 9, 19–46.

Schleifer, A., Vishny, R.W., 1997. The limits of arbitrage. Journal of Finance 52, 35–55.

Schwert, G.W., 2003. Anomalies and market efficiency, in: Constantinides, G.M., Harris, M., Stulz, R.M. (Eds.), Handbook of the Economics of Finance. North Holland.

Sharpe, W.F., 1964. Capital asset prices: A theory of market equilibrium under conditions of risk. Journal of Finance 19, 425–442.

Souza, T.d.O., 2020. Price of risk fluctuation and the size premium. Working paper, University of Southern Denmark .

Todorov, V., Bollerslev, T., 2010. Jumps and betas: A new framework for disentangling and estimating systematic risks. Journal of Econometrics 157, 220–235.

Wachter, J.A., 2013. Can time-varying risk of rare disasters explain aggregate stock market volatility? Journal of Finance 68, 987–1035.